J. Chem. Thermodynamics 164 (2022) 106618

Contents lists available at ScienceDirect

J. Chem. Thermodynamics

journal homepage: www.elsevier.com/locate/jct

Measurement of the density of carbon dioxide/toluene homogeneous mixtures and correlation with equations of state

Hiroaki Matsukawa [a], Tomoya Tsuji [b], Katsuto Otake [a,*]

[a] Department of Industrial Chemistry, Faculty of Engineering, Tokyo University of Science, Ichigaya funagawaramachi 12-1, Shinjuku Ku, Tokyo 162-0826, Japan
[b] Malaysia Japan International Institute of Technology, Universiti Technologi Malaysia, Off Jalan Sultan Yahya Petra, Kuala Lumpur 54100, Malaysia

ARTICLE INFO

Article history:
Received 31 March 2021
Received in revised form 16 August 2021
Accepted 17 August 2021
Available online 22 August 2021

Keywords:
Density
Carbon dioxide
Toluene
Peng-Robinson equation of state
Sanchez-Lacombe equation of state
PC-SAFT equation of state

ABSTRACT

Equations of state (EoS) can be used to estimate a wide variety of physical properties. However, there has been limited verification of the applicability of parameter sets derived from specific physical properties to correlate and estimate various other physical properties. The densities of homogeneous phase fluid mixtures of the carbon dioxide (CO_2)/toluene (Tol) binary system were measured and correlated to three equations of state. The density measurements were performed using a high-pressure vibration-type density meter equipped with a circulation pump and variable-volume viewing cell, which guaranteed the homogeneity of the mixtures. The densities were measured at temperatures ranging from 313 to 353 K, pressures up to 20 MPa, and CO_2 concentrations from 0 to 80 mol%. The experimental data obtained were correlated to the Tait density equation and three EoS, namely Peng–Robinson (PR), Sanchez–Lacombe (SL), and Perturbed Chain statistical associating fluid theory (PC-SAFT) EoS. Among them, SL and PC-SAFT EoS agree better with the experimental data compared to the PR EoS, presumably due to differences in the pure component parameters used in each EoS. Using parameter sets determined from the density measurements, the vapor liquid equilibrium (VLE) of the CO_2/Tol mixtures was estimated. While we were unsuccessful in estimating VLE using the PR EoS, SL and PC-SAFT EoS were successfully used for the estimations. We also attempted to determine the densities from VLE correlations. It was found that SL and PC-SAFT EoS could be used to estimate the density well, whereas the PR was not predictive. From the results of the study, it is clear that for estimating density using EoS, the basic data used for determining the pure component parameters are important.

1. Introduction

In recent years, there have been many attempts to employ supercritical carbon dioxide ($scCO_2$) as an alternative solvent and/or reactant owing to its mild critical properties, excellent diffusivity, solubility, non-reactivity, non-toxic nature, and low cost. In addition, $scCO_2$ can be easily removed from solutions by depressurization and/or cooling, making it an attractive solvent. It can be employed in various industrial processes such as extraction [1], drying [2], and particle synthesis [3]. For example, $scCO_2$ is used in the extraction of toluene (Tol) from heavy oil [4] or for drying during the preparation of aerogels [5]. However, using pure $scCO_2$ on its own as a solvent has certain limitations such as low solubility of target compounds. Therefore, binary mixtures of $scCO_2$ and organic solvents are being considered for dissolving various compounds that are not readily soluble in pure $scCO_2$. Generally, these mixtures are formed by combining $scCO_2$ with organic solvents such as alcohols, alkanes, and cycloalkanes. For example, solvent mixtures composed of CO_2 and cyclohexane (C_6H_{12}) or Tol have attracted significant attention for various polymer applications, particularly for the extraction and preparation of polymers or as processing fluids for polyolefins [6,7]. In order to design effective industrial processes, the physical properties of mixed solvent systems, such as vapor–liquid equilibrium (VLE) and density, need to be considered. For example, reliable values of density, which typically reflects the mixing characteristics, are important for understanding the change in the solvent characteristics due to mixing during a process. Moreover, the phase of the CO_2/organic solvent system changes with temperature, pressure, and composition. Therefore, it is important to understand the phase state in which the density of the solvent mixture is measured. Fig. 1 shows the VLE diagram of the CO_2/Tol system [8]. In the figure, the solid lines represent VLE of the binary system calculated using the Peng–Robinson equation of state (PR EoS) [9]. For detailed process design, the properties of the mixtures in the homogeneous regions

* Corresponding author.
E-mail address: k-otake@ci.kagu.tus.ac.jp (K. Otake).

https://doi.org/10.1016/j.jct.2021.106618
0021-9614/

Nomenclature

T	temperature, K
P	pressure, Pa or MPa
V	molar volume, m^3/mol
ρ	density, kg/m^3
Z	compressibility factor
f	fugacity, Pa
φ	fugacity coefficient
μ	chemical potential, J
A	Helmholtz free energy, J
T_c	critical temperature, K
P_c	critical pressure, Pa or MPa
ω	acetic factor
x_i	mole fraction of component i
w_i	mass fraction of component i
ϕ_i	volume fraction of component i
R	gas constant, J/(mol K)
k	Boltzmann constant, J/K
N_{data}	number of data points

Peng-Robinson equation of state

a	energy parameter
b	volume parameter
$T_r = T/T_c$	reduced temperature
k_{ij}, l_{ij}	interaction parameter

Sanchez-Lacombe equation of state

$\tilde{T}, \tilde{P}, \tilde{\rho}$	reduced parameter
T^*	characteristic temperature, K
P^*	characteristic pressure, MPa
ρ^*	characteristic density, kg/m^3
V^*	characteristic volume, m^3/mol
r	segment number
δ_{ij}	interaction parameter

Perturbed-Chain SAFT equation of state

$\tilde{a}$	reduced Helmholtz free energy
m	number of segments per chain
σ	segment diameter, Å
d	temperature-dependent segment diameter, Å
ε	depth of pair potential, J
N	total number of molecules
ζ_n	abbreviation ($n = 0, ..., 3$) defined by *Eq.* (30), Å
I_1, I_2	abbreviation
η	packing fraction,$\eta = \zeta_3$
g^{hs}	radial distribution function of the hard-sphere fluid
ρ_m	total number density of molecules, 1/Å^3
θ_{ij}	interaction parameter

Superscripts

cal	calculated property
exp	experimental property
hc	residual contribution of hard-chain system
hs	residual contribution of hard-sphere system
disp	dispersion contribution
assoc	association contribution

(areas outside VLE in Fig. 1) are very important. While there are many literature reports describing VLE and saturated liquid phase density (i.e., the density along the VLE lines) of CO_2/organic solvent systems, data on the fluid density in the homogeneous phase area is limited for these systems. For example, Zirrahi *et al.* [10] reported the solubility and density of the saturated liquid phase for a CO_2/Tol system. We measured the density of homogeneous phase fluid mixtures of CO_2/cyclohexane (C_6H_{12}), CO_2/methyl cyclohexane ($C_6H_{11}CH_3$), and CO_2/ethyl benzene ($C_6H_5C_2H_5$) systems and investigated the effect of the molecular structure on the density[11].

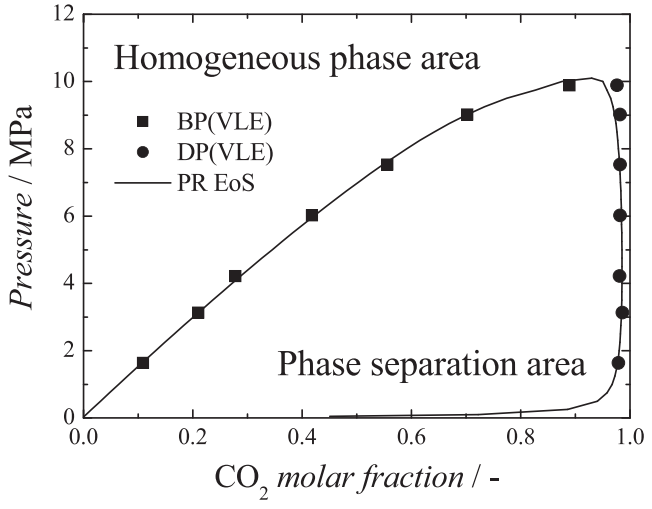

Fig. 1. Vapor-liquid equilibrium diagram of the CO_2/Tol system at 333 K [8].

As physical property measurements require specialized equipment and long acquisition periods, experimental data reported in the literature are often insufficient and limited. Therefore, the estimation of physical properties through calculations is an important supplementary method to experimental measurements. In systems that are under high pressure such as mixtures containing $scCO_2$, the equation of state (EoS) is powerful for estimating physical properties. EoS is often used to calculate VLE and solubility because it not only describes the basic pressure-volume-temperature relationships of a system, but also allows the calculation of thermodynamic parameters such as Gibbs free energy and enthalpy. Many types of EoSs are available. At present, all available EoSs can be classified into three main types, namely, based on van der Waals, lattice fluid, and perturbation theory. Heretofore, attempts have been made to select an appropriate EoS for reliably estimating a certain physical property. For example, if one only wants to calculate density, one can use a density correlation equation such as the Tait equation. However, chemical process design requires not only density, but also various other physical properties such as phase equilibrium characteristics. Therefore, using only specialized equations to estimate specific physical properties is very inefficient. In order to apply EoS to obtain various physical properties, it would be desirable to be able to correlate and estimate as many properties as possible from appropriate parameter sets, determined from a simple single set of experimental data. However, there has been limited verification of the validity of applying parameter sets obtained from specific physical properties, to correlate and estimate various other physical properties. Moine *et al.* [12] compared the Soave-Redlich-Kwong EoS (SRK EoS, one of the van der Waals EoS) [13] and the perturbed chain statistical associating fluid theory EoS (PC-SAFT EoS) [14,15] for estimating the physical properties of pure components. They pointed out that due to the

difference in the parameterization method for pure component parameters, the SRK EoS failed in accurately reproducing liquid density [16,17] and the PC-SAFT EoS overestimated critical pressure [18]. Further, they also suggested that the unification of the parameterization method for pure component parameters that involved the combined analysis of saturated vapor pressure and liquid density results in no significant difference in the accuracy of the estimation of various physical properties between the two EoSs. To overcome the shortcoming of the van der Waals EoS, that is, the inaccurate estimation of the density of the liquid, a method called volume translation has been proposed to add a correction term to density [19,20]. Mallepally *et al.* [21] compared the SRK EoS, PC-SAFT EoS, and modified Sanchez-Lacombe EoS (MSL EoS, one of the lattice fluid EoS) [22,23] for estimating the phase behavior and densities of propylene/toluene and ethylene/toluene systems. MSL EoS is the modification of Neau's version of the Sanchez-Lacombe EoS (SL EoS) [24–26] in that it includes a Péneloux-type volume translation. It was reported that both SRK and PC-SAFT EoSs facilitate the accurate estimation of the phase behavior and densities of various systems; however, they slightly overpredicted the densities.

In this work, the densities of homogeneous phase fluid mixtures of the CO_2/Tol system were measured at temperatures ranging from 313 to 353 K and pressures up to 20 MPa using a high-pressure vibration-type density meter. By considering a system containing Tol, we could determine the differences in aromatic- and *cyclo*-rings of C7 compounds and/or alkyl chain length upon comparison with previously reported systems [11]. The CO_2 composition was varied from 0 to 80 mol% at 20 mol% intervals. The experimental data obtained were correlated to the Modified Tait density equation [27] and the three EoSs, namely, PR [9], SL [24–26], and PC-SAFT [14,15]. Using the parameter sets obtained from each of the three EoSs, the VLE of the CO_2/Tol system was estimated. Further, the validity of the parameter sets obtained by correlating the density and VLE data and *vice versa* was discussed, and the difference in the estimation accuracy for the densities and phase behavior by the basic calculation method of each EoS was determined.

2. Experimental

2.1. Materials

Carbon dioxide (CO_2, CAS number [124–38–9], mass fraction purity >99.99%) was purchased from Showa Yozai Co. Ltd. Toluene ($C_6H_5CH_3$, CAS number [108–88–3], mass fraction purity >99.5%) was obtained from Kanto Kagaku Co. All the reagents were used as received. The specifications of pure CO_2 and Tol are listed in Table 1.

2.2. Apparatus and procedure

In this study, the density of the homogeneous phase of the CO_2/Tol binary mixture was measured with an experimental apparatus containing a variable-volume viewing cell (Tamaseiki Ind. Co., H-050151-1), high-pressure vibration-type density meter (Anton Paar Co., DMP 512), and circulation pump (Nihon Seimitsu Kagaku Co., Ltd., NP-AX-20(J)). In addition, it was equipped with a piston head temperature controller and constant temperature air bath (Yamato Scientific Co., Ltd., DKN602). The high-pressure vibration type density meter measured the oscillation period of the U-tube, which contained the sample. The following equation was used to determine the densities from the measured period of oscillation [28].

$$\rho = A\tau 2 - B \quad with \begin{cases} A = a + bP + cP2 \\ B = d + eP + fP2 \end{cases} \tag{1}$$

where ρ, P, and τ are the density, pressure, and oscillation periods, respectively, and a, b, c, d, e, and f are the apparatus constants. In order to determine the values of these constants, two samples of known density need to be measured at the experimental pressure and temperature. In this work, the REFPROP ver. 10 values of water and Tol were used as reference samples of known density. The temperature dependence was not considered due to the lack of measurement data. Therefore, the apparatus constants were determined at each temperature. The details of the experimental apparatus and procedures employed have been described elsewhere [11,29]. The homogeneity of the phase was confirmed from the VLE phase diagram as well as visual observation through the viewing window of the variable-volume viewing cell.

For all the measurements, the temperature and pressure uncertainties were ± 0.15 K and ± 0.033 MPa, respectively. The combined standard uncertainties in the composition and experimental density values were calculated for each data point. Details of the calculation methods have been described previously [11].

2.3. Experimental data correlations and estimation of density

2.3.1. Density equation

In this study, the experimental data were fit to the Modified Tait equation shown in Eq. (2) [27]:

$$\rho = \frac{\rho_2^{0*} + ax_1 \frac{1+bx_1+cx_1^2}{1+mx_1+nx_1^2}}{1 - k\ln\left\{1 - \frac{1-(P/P^*)}{1+\exp[A-B/(C-x_1)]}\right\}} \tag{2}$$

where ρ, x, and P are the density, molar fraction, and pressure, respectively. Superscripts 0 and * represent the pure component and reference, respectively. P^* is the reference pressure at the highest pressure. Subscripts 1 and 2 represent carbon dioxide and organic solvent, respectively. The nine parameters, a, b, c, m, n, A, B, C, and k, are the fitting parameters in *Eq.* (2), and are not dependent on the composition. The details of the correlation method have been described elsewhere [11].

2.4. PR EoS

The van der Waals EoS is applicable for an ideal gas with correction terms for volume and energy. The PR EoS is currently the most commonly used equation of this type. In this study, the experimental data were correlated with the PR EoS shown below [9]:

$$P = \frac{RT}{V-b} - \frac{a(T)}{V(V+b)+b(V-b)} \tag{3}$$

where V and R are the molar volume and gas constant, respectively, and $a(T)$ and b are the PR EoS parameters. The pure component

Table 1
Specifications of pure components.

Component	CAS number	M_W/mol g^{-1}	Supplier	Mass fraction purity (Supplier)
Carbon dioxide, CO_2	124–38-9	44.01	Showa Yozai Co.	0.9999
Toluene, $C_6H_5CH_3$, Tol	108–88-3	92.14	Kanto Kagaku Co.	0.995

parameter $a(T)$, which is a function of temperature, and b are given by the following equations.

$$a(T) = \alpha \cdot a(T_c) \tag{4}$$

$$\alpha^{1/2} = 1 + \kappa\left(1 - T_r^{1/2}\right) \tag{5}$$

$$\kappa = 0.37464 + 1.54226\omega - 0.26992\omega^2 \tag{6}$$

$$a(T_c) = 0.45724\frac{R^2 T_c^2}{P_c} \tag{7}$$

$$b = 0.07780\frac{RT_c}{P_c} \tag{8}$$

where T_c, P_c, and T_r represent the critical temperature, critical pressure, and reduced temperature, respectively. The parameter κ is defined in terms of the acentric factor ω. Thus, the pure component parameters for the PR EoS are the critical temperature, critical pressure, and ω.

To calculate the properties of solvent mixtures, mixing rules are employed. There are several mixing rules available for the various EoS. In this study, we used typical mixing rules for each of the EoS. For the PR EoS, the van der Waals' one-fluid mixing rule was employed [30].

$$a = \sum_i \sum_j x_i x_j (1 - k_{ij}) (a_i a_j)^{1/2} \tag{9}$$

$$b = \sum_i \sum_j x_i x_j (1 - l_{ij}) \frac{b_i + b_j}{2} \tag{10}$$

where x_i is the molar fraction of the i^{th} component, a_i and b_i are the PR EoS parameters of the i^{th} pure component, and k_{ij} and l_{ij} are the binary interaction parameters for the i-j pair, respectively. a_i, b_i, k_{ij}, and l_{ij} are the fitting parameters.

The critical properties and acentric factors, which are pure component parameters in the PR EoS, are listed in Table 2 [31].

2.4.1. SL EoS

The lattice-fluid type EoS is derived from the Flory–Huggins theory. It is mainly used to study polymeric solutions and is applicable to large-molecule systems such as macromolecules because it does not require a critical value as a pure parameter. In this study, the experimental data were correlated to SL EoS, which is a lattice fluid-type EoS, and is shown below [24–26]:

$$\tilde{\rho}^2 + \tilde{P} + \tilde{T}\left\{\ln\left(1 - \tilde{\rho}\right) + (1 - 1/r)\,\tilde{\rho}\right\} = 0 \tag{11}$$

where $\tilde{P}$, $\tilde{T}$, and $\tilde{\rho}$ are the reduced pressure, temperature, and density, respectively, and r is the size parameter that represents the number of lattice sites occupied by a molecule. The reduced parameters for a pure substance are defined as

$$\tilde{T} = T/T^* \; \tilde{P} = P/P^* \; \tilde{\rho} = \rho/\rho^* = V^*/V \tag{12}$$

$$r = P^* V^*/RT^* \tag{13}$$

where P^*, T^*, and ρ^* are the SL EoS characteristic parameters and M is the molecular weight. The characteristic parameters are defined as follows:

$$T^* = \varepsilon^*/kP^* = \varepsilon^*/v^*\rho^* = M/rv^* \tag{14}$$

where ε^* and v^* are the segment interaction energy and segment volume, respectively. A pure component can be completely characterized by three EoS parameters, namely, P^*, T^*, and v^* (or equivalently, ρ^*). These pure component parameters for SL EoS were obtained by correlating the PVT data.

The mixing rule for SL EoS used in this study is described by the following set of Eq. [32].

$$\frac{1}{V^*} = \sum_i \frac{\phi_i}{V_i^*} \tag{15}$$

$$\phi_i = \frac{w_i/\rho_i^*}{\sum_j w_j/\rho_j^*} \tag{16}$$

$$P^* = \sum_i \phi_i P_i^* - RT \sum_j \sum_{i<j} \phi_i \phi_j \chi_{ij} \tag{17}$$

$$\chi_{ij} = \frac{P_i^* + P_j^* - 2(1 - \delta_{ij})\left(P_i^* P_j^*\right)^{1/2}}{RT} \tag{18}$$

$$T^* = \frac{P^* v_0}{R} \tag{19}$$

$$\frac{1}{v_0} = \sum_i \phi_i \left(\frac{P_i^*}{RT_i^*}\right) \tag{20}$$

where φ_i and w_i are the close-packed volume fraction and mass fraction of the i^{th} component, respectively, and δ_{ij} is the i-j interaction parameter. As in the case of the PR EoS, the interaction parameters were used as fitting parameters in the correlation. The characteristic parameters, which are the pure component parameters used in this study, are summarized in Table 2 [25].

2.4.2. PC-SAFT EoS

The SAFT-type EoS is derived from the perturbation theory. Perturbation theory is a methodology for obtaining solutions by adding perturbation terms to the main solution. It is based on the statistical thermodynamic treatment of aggregation by

Table 2
Pure component parameters for the three EoS.

Peng-Robinson equation of state				
	P_c/MPa	T_c/K	ω	Ref.
CO_2	7.38	304.1	0.225	[31]
Toluene	3.47	572.2	0.237	[31]
Sanchez-Lacombe equation of state				
	P^*/MPa	T^*/K	ρ^*/kg m^{-3}	Ref.
CO_2	574.5	305	1510	[25]
Toluene	397	543	966	[25]
PC-SAFT equation of state				
	m	σ/A	$\varepsilon\, k^{-1}$/K	Ref.
CO_2	2.0729	2.7852	169.21	[14]
Toluene	2.8149	3.7169	285.69	[14]

Wertheim and is used to represent the PVT relations of fluids. In this study, the experimental data were correlated with the PC-SAFT EoS, which is representative of the SAFT-type EoS, shown below [14,15]:

$$\frac{A^{res}}{NkT} = \tilde{a}^{res} = \tilde{a}^{hc} + \tilde{a}^{disp} + \tilde{a}^{assoc} \tag{21}$$

where A^{res} is the residual Helmholtz free energy, and $\tilde{a}^{hc}$, $\tilde{a}^{disp}$, and $\tilde{a}^{assoc}$ are contributions to the Helmholtz free energy by a chain of hard spheres, by diffusion, and association, respectively. Association is not expected to occur between the components in this study, and thus, the contribution by association can be ignored. The compression factor Z is expressed in terms of the Helmholtz free energy as shown in Eq. (22):

$$Z = 1 + \eta\left(\frac{\partial \tilde{a}^{res}}{\partial \eta}\right)_{T,x_i} \tag{22}$$

where η is the packing fraction. The contributions to the Helmholtz free energy from the chain of hard spheres and by diffusion are as follows:

$$\tilde{a}^{hc} = \bar{m}\,\tilde{a}^{hs} - \sum_i x_i(m_i - 1)\ln g_{ii}^{hs}(\sigma_{ii}) \tag{23}$$

$$\tilde{a}^{disp} = -2\pi\rho_m I_1\left(\eta,\bar{m}\right) m^2\bar{\varepsilon}\sigma^3 - \pi\rho_m \bar{m}\, C_1 I_2\left(\eta,\bar{m}\right) m^2\bar{\varepsilon}^2\sigma^3 \tag{24}$$

$$\bar{m} = \sum_i x_i m_i \tag{25}$$

$$m^2\bar{\varepsilon}\sigma^3 = \sum_i\sum_j x_i x_j m_i m_j\left(\frac{\varepsilon_{ij}}{kT}\right)\sigma_{ij}^3 \tag{26}$$

$$m^2\bar{\varepsilon}^2\sigma^3 = \sum_i\sum_j x_i x_j m_i m_j\left(\frac{\varepsilon_{ij}}{kT}\right)^2\sigma_{ij}^3 \tag{27}$$

$$\rho_m = \frac{6}{\pi}\left(\sum_i x_i m_i d_i^3\right)^{-1} \tag{28}$$

where m, σ, and ε are the number of segments per chain, segment diameter, and depth of the pair potential, respectively. $\bar{m}$ is the average number of segments per chain and ρ_m is the total number density of molecules. $\tilde{a}^{hs}$, which is the contribution to the Helmholtz free energy by hard spheres, is given by Eq. (29).

$$\tilde{a}^{hs} = \frac{1}{\zeta_0}\left[\frac{3\zeta_1\zeta_2}{1-\zeta_3} + \frac{\zeta_2^3}{\zeta_3(1-\zeta_3)^2} + \left(\frac{\zeta_2^3}{\zeta_3^2} - \zeta_0\right)\ln(1-\zeta_3)\right] \tag{29}$$

In addition, g_{ij}^{hs} is the radial distribution function of the hard-sphere fluid and is given by Eq. (30):

$$g_{ij}^{hs} = \frac{1}{1-\zeta_3} + \left(\frac{d_i d_j}{d_i + d_j}\right)\frac{3\zeta_2}{(1-\zeta_3)^2} + \left(\frac{d_i d_j}{d_i + d_j}\right)^2\frac{2\zeta_2^2}{(1-\zeta_3)^3} \tag{30}$$

where ζ_n is defined as

$$\zeta_n = \frac{\pi}{6}\rho_m\sum_i x_i m_i d_i^n n \in \{0,1,2,3\} \tag{31}$$

Finally, d is the temperature-dependent segment diameter and is given by Eq. (32).

$$d_i = \sigma_i\left[1 - 0.12\exp\left(-3\frac{\varepsilon_i}{kT}\right)\right] \tag{32}$$

In the above equations, the three pure component parameters of the PC-SAFT EoS are m, σ, and ε. These parameters were obtained by fitting the experimental liquid density and vapor pressure of the pure components to the PC-SAFT EoS.

The following mixing rule for the PC-SAFT EoS was used in this study [14]:

$$\sigma_{ij} = \frac{1}{2}(\sigma_i + \sigma_j) \tag{33}$$

$$\varepsilon_{ij} = (1 - \theta_{ij})\sqrt{\varepsilon_i\varepsilon_j} \tag{34}$$

where θ_{ij} is the interaction parameter and is a fitting parameter in the correlation. The PC-SAFT EoS parameters, which are the pure component parameters used in this study, are summarized in Table 2 [14].

3. Results and discussion

3.1. Density of the CO_2/Tol system

Experimental measurements of the density of the CO_2/Tol system are shown in Figs. 2–4 and 6 and Table 3. Fig. 2(a) shows a comparison of the density of pure Tol with the literature data [33–35,28]. The solid line in the figure is REFPROP values. Fig. 2 (b) depicts the deviations of this work and literature data relative to REFPROP values. As shown in the figures, the experimental and literature data agree well. Thus, it can be concluded that the experimental apparatus is sufficiently reliable for this measurement.

Fig. 3(a) and (b) show the density–pressure and density–composition relationships, respectively, for the CO_2/Tol system. The density of pure CO_2 was calculated using the EoS proposed by Span and Wagner [36]. From Fig. 3(a), at low CO_2 concentrations, the density of the CO_2/Tol system increases with increasing CO_2 mole fraction, whereas it decreases (approaching the density of pure CO_2) at higher CO_2 concentrations. This tendency can be explained by the fact that at low CO_2 concentrations, the penetration of CO_2 between the organic molecules makes the mixture dense. In contrast, at high CO_2 compositions, the organic molecules are surrounded by CO_2, as a result of which the properties of CO_2 become dominant. This is similar to the trends observed for CO_2/organic solvent (C_6H_{12}, $C_6H_{11}CH_3$, and $C_6H_5C_2H_5$) mixtures studied previously [11].

Fig. 3(b) shows the effect of temperature on the CO_2/Tol system. The density data in Figs. 3-5 is an interpolation of Table 3. In general, the density decreases with increasing temperature, with a particularly high rate of decrease at high CO_2 concentrations. This observation could be related to the thermal expansion characteristics of the mixture. The thermal expansion coefficient α_p of CO_2 is 0.010 K^{-1} (at 12 MPa, 300 K) [38], while that of Tol is much lower at 1.015×10^{-3} K^{-1} (at 9.27 MPa, 304.1 K) [37]. Thus, the densities of mixtures with high CO_2 concentrations are drastically different compared to those for mixtures with low CO_2 concentrations, since the properties of CO_2 become dominant as its mole fraction increases. A similar tendency was observed for systems measured in previous studies.

Fig. 4 shows the experimental values of the density for the CO_2/Tol system obtained in this study with literature data[39–41]. The density data at 15 MPa in the figure are obtained by interpolation of Table 3 and literature data. The trend of density change against composition in this work and literature data was consistent.

In Fig. 5, the CO_2/Tol system at 313 K is compared to the CO_2/methylcyclohexane ($C_6H_{11}CH_3$, MC) and CO_2/ethylbenzene ($C_6H_5C_2H_5$, EB) systems measured in a previous study [11]. From both Fig. 5 (a) and (b), both mass and mole density of pure Tol

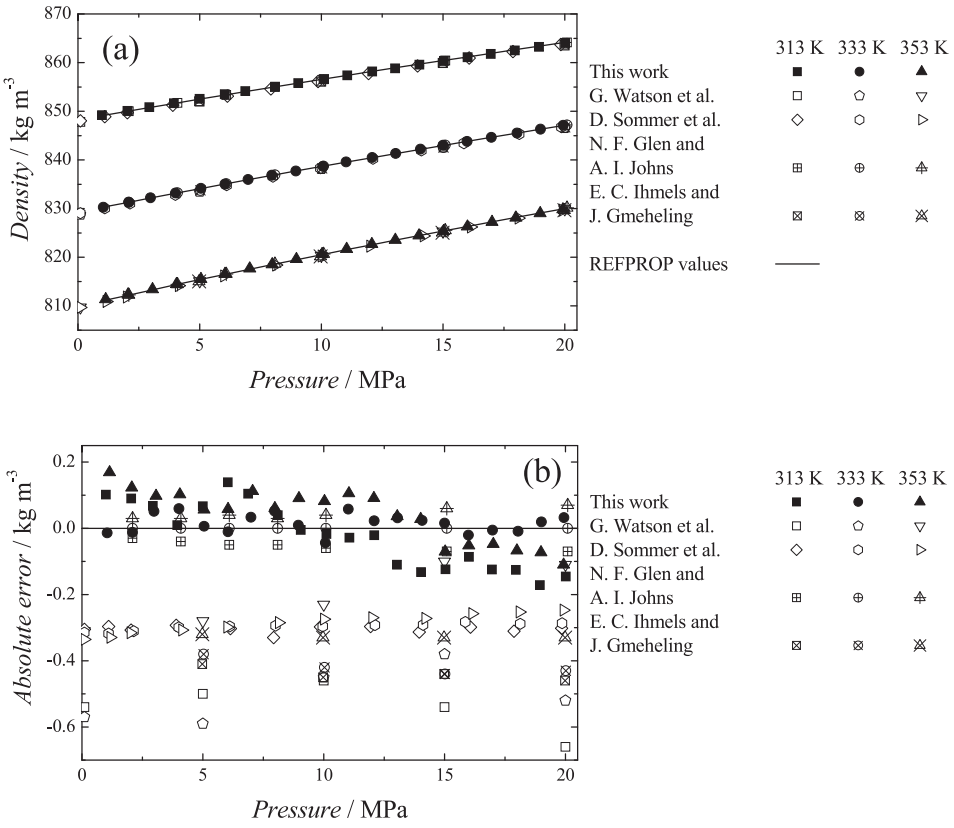

Fig. 2. Comparison of the density of pure Tol measured in this work against previously reported results [32–35]: (a) density-pressure correlations of the experimental results, (b) variations in deviation of density with pressure.

are higher than those of MC and slightly higher than those of EB. In addition, among the three solvents, MC is the most sensitive to mass density changes as a function of CO_2 composition. In contrast, there was no difference in the mole density changes as a function of CO_2 composition. The van der Waals volumes of Tol, EB, and MC, calculated using Bondi's method [41], were 59.51, 69.74, and 71.6 $cm^3\ mol^{-1}$, respectively — these volumes were almost equal for EB and MC, with the van der Waals volume of Tol being significantly smaller than those of the other two solvents. This was in agreement with the trend of molar density shown in Fig. 5(b). Furthermore, the partial molar volume was calculated using the density equation, and has been shown in Fig. 6 for conditions of 313 K and 10 MPa. As described above, partial molar volume could not be calculated over the entire spectrum of composition because the density equation used has the limitation of being applicable only at certain compositions. The partial molar volume of each component in the CO_2/MC system was the largest of the three systems. Additionally, the trend of the free volume of the organic solvent was also similar to that of its van der Waals volume. The relationship between the CO_2 concentration and density in the CO_2/MC system can be explained based on the delocalization of π electrons on the benzene ring, which shortens the C—C bond lengths of Tol and EB more compared to that of MC. Therefore, MC is the bulkiest among the three solvents and hence has the lowest density. In contrast, the difference in the number of –CH_2- entities between the methyl and ethyl groups makes EB slightly bulkier, which explains the lower density of EB compared to that of Tol.

The absolute average relative deviation (*AARD*) for density given below was optimized by changing the fitting parameters of the density equation.

$$AARD = \frac{100}{N_{data}} \sum \left| \frac{\rho_{cal} - \rho_{\exp}}{\rho_{\exp}} \right| \tag{35}$$

where N_{data} denotes the number of data points, whereas the subscripts *cal* and exp denote the calculated and experimental values, respectively. Table 4 shows the parameter values obtained by correlations using the density equation. The density-pressure and density-composition relationships for the fits obtained with the density equation are also shown in Fig. 3 as solid lines. It is clear from Table 4 and Fig. 3 that the calculated values agree well with the experimental values. Further, the *AARD* of the correlation was approximately 0.2%. The effective CO_2 composition of the Modified Tait equation used is assumed to be less than 0.95 in the literature [27]. The effective CO_2 molar fraction range for the determined parameters was from 0 to about 80 mol% due to the CO_2 composition range of the correlated experimental data. As previously reported [11], the parameters were not found to be dependent on temperature. However, it should be noted that the parameters strongly depended on the initial values.

3.2. Correlation of density with EoS

The parameters and *AARD* obtained by correlating the experimental density values with the three EoS are tabulated in Table 5 and the fit curves are shown in Fig. 7. From the table and figure, it can be seen that SL and PC-SAFT EoS show similar *AARD* and identical correlation results, whereas PR EoS exhibits high *AARD* values and a large discrepancy with the other two models. Thus, it can be concluded that SL and PC-SAFT EoS correlate well with the density of homogeneous mixtures, but PR EoS does not. This can be explained by the difference in the accuracy of estimating the density of the pure components. As seen from Fig. 7, PR EoS

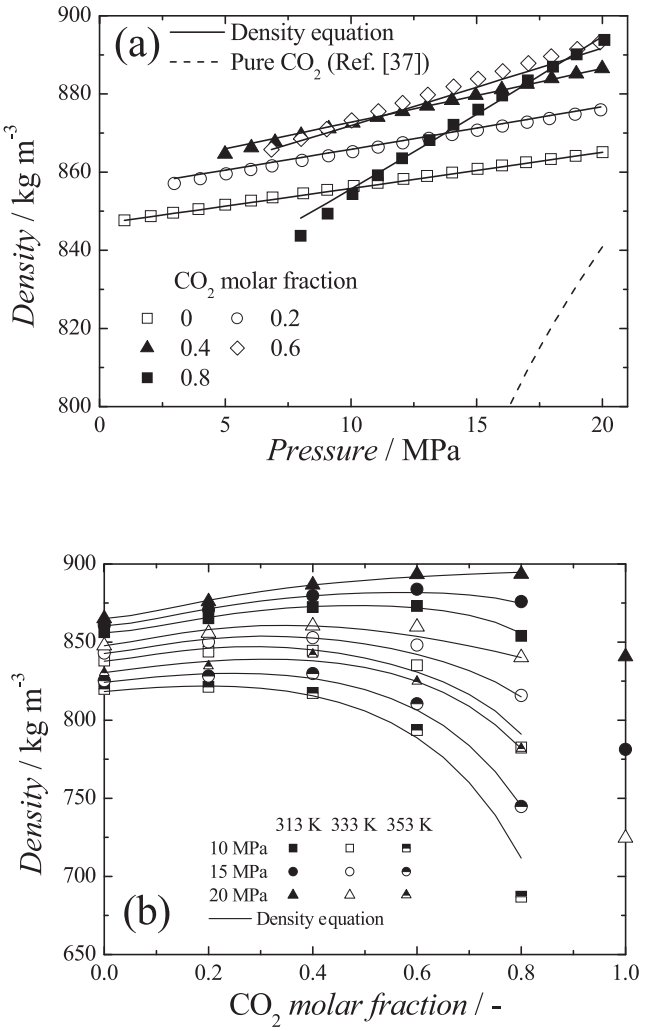

Fig. 3. Density behavior of the CO_2(1)/Tol(2) system. (a) Pressure dependence at 313 K, (b) CO_2 mole fraction dependence, pure CO_2 values are from Ref. [28].

does not exhibit good correlation to the density of pure Tol, while SL and PC-SAFT EoS show good agreement. In contrast, in the case of the PR EoS correlation, the initial discrepancy of the pure component density cannot be corrected by introducing the interaction parameter for the mixture, which is a fitting parameter, and the fit curve is different from the experimental data.

This difference in the accuracy of estimating the densities of pure components can be explained by the difference in the pure component parameters required by the individual EoS. In the PR EoS, the critical constants and acentric factor are used as the pure component parameters. In contrast, the pure component parameters for SL EoS are obtained by correlating PVT data, whereas those for the PC-SAFT EoS are obtained by correlating the liquid density and saturated vapor pressure. Therefore, the accuracy of estimating the densities of the pure components using these two EoS is naturally better than that of the PR EoS.

In contrast with an ideal gas, real fluids have finite molecular volumes and exhibit intermolecular interactions. To represent these effects, the EoS for real fluids contain attractive and repulsive terms. Over the course of development of the van der Waals EoS, modifications have been made to the attractive term, whereas no modifications have been made to the repulsive term. The hard sphere potential and potential of a real gas are reported to agree relatively well, and the energy state of the solution is dominated by the effect of intermolecular repulsion as compared to attraction [16]. In the case of the PR EoS, the excluded volume *b* is determined by the critical value and remains unaffected by pressure or temperature. Therefore, it could be treated as a hard sphere. However, because it is a very simple approximation, the excluded volume obtained from the critical value cannot accurately represent the repulsion between molecules. In fact, it was reported that the repulsive term in the van der Waals EoS considerably differs from that in real gases. Fukuchi *et al.* [17] compared the compression factor of a real gas calculated by simulations with that calculated by van der Waals EoS, and found that the bias is larger in the high-density region. This may be due to the overlap of the free volume of molecules, which makes it impossible to model the behavior of real fluids.

It is possible to improve the accuracy in estimating the densities of the pure components in the PR EoS by volume translation [19,20], although inherent defects make the PR EoS inappropriate for the calculation and correlation of densities. Since the purpose of this study was to discuss the fundamental calculations pertaining to each EoS, no calculations involving volume translation were performed. In contrast, the PC-SAFT EoS, which is based on a hard sphere, would be suitable for density calculations, considering the characteristics of the equation. Similarly, SL EoS, which is

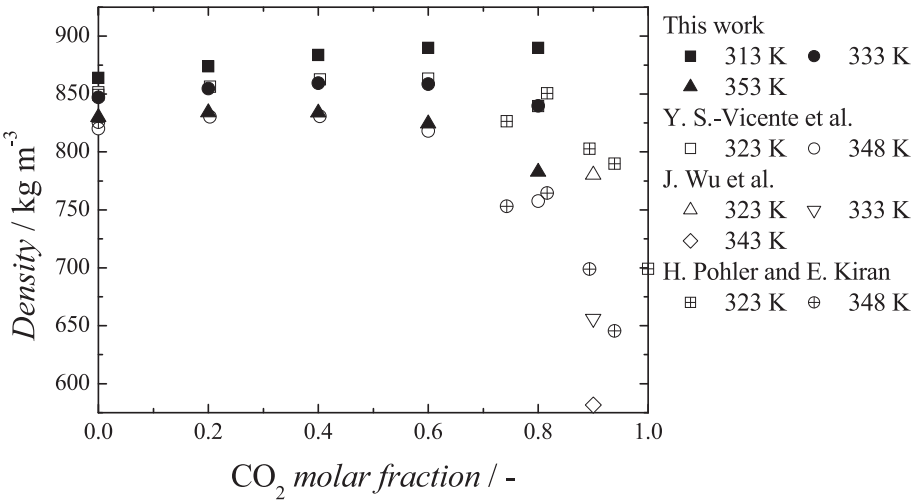

Fig. 4. Comparison of the density of the CO_2(1)/Tol(2) mixture measured in this work against previously reported results [39–41] at 15 MPa.

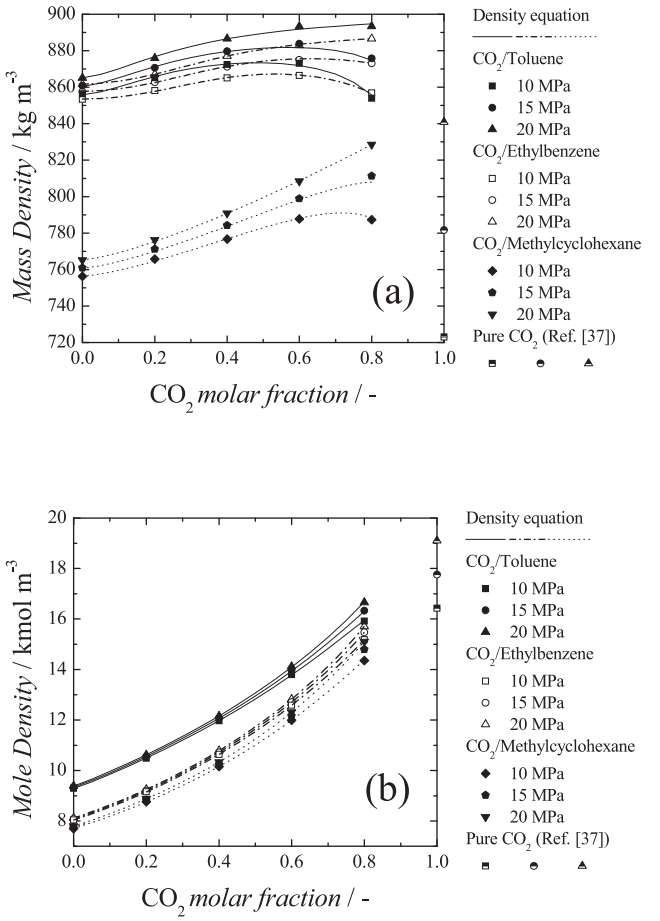

Fig. 5. Comparison of the density behavior of the CO_2(1)/Tol(2) and CO_2(1)/organic solvent(2) systems measured in a previous study [11] at 313 K. (a) Mass density and (b) mole density.

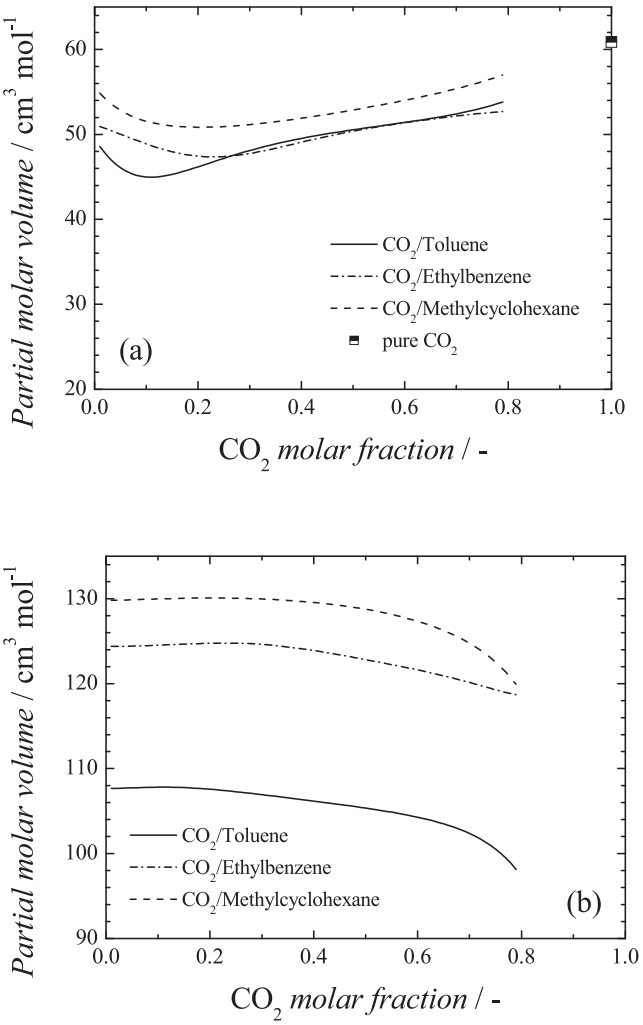

Fig. 6. Comparison of the partial molar volume of (a) CO_2 and (b) organic solvent in CO_2(1)/Tol(2) and CO_2(1)/organic solvent(2) systems at 313 K and 10 MPa, measured in a previous study [11].

formulated from the lattices that take into account the free volume change, is also expected to be applicable for density calculations.

3.3. Estimation of VLE with EoS

The VLE line of the CO_2/Tol system was estimated using the various EoS with the interaction parameters obtained using the density correlations. The estimated results are shown in Table 6 and Fig. 8 and were evaluated using the *AARD* calculated by the following equation as well as literature values [8,43–45].

$$AARD = \frac{100}{N_{data}} \sum \left| \frac{x_{1,cal} - x_{1,\exp}}{x_{1,\exp}} \right| \tag{36}$$

where x_1 is the CO_2 mole fraction.

The interaction parameters in each EoS represent the differences in structure and energy between the component molecules, and not the physical properties. Ideally, the VLE line can be estimated using the parameters obtained from the density correlations. From the table, the *AARD* decreases in the following order: PR EoS $\gg$ SL EoS > PC-SAFT EoS. As mentioned, the PR EoS parameters determined in the previous section are not reliable and therefore, result in a large error in the VLE estimations. Adachi *et al.* [46] mathematically examined the effect of the energy term in the van der Waals EoS on the calculation of the vapor pressure of pure components as well as the VLE of a binary system. In the van der Waals EoS, when a simple mixing rule is applied, the change in excluded volume *b*, which is important for the density calculations, had no effect on the accuracy of VLE estimation. In other words, the fugacity coefficient necessary for the calculation of VLE depends only on the temperature, pressure, and energy parameter, *a*. They concluded that there is no relationship between the accuracy in estimating VLE and the accuracy of estimating the density because the parameters on which the calculation relies are different. In Fig. 8, the solid and dashed lines are the estimation results obtained using SL EoS and PC-SAFT EoS, respectively. The PR EoS, which could not be used for clear estimations, is not considered in Fig. 8. The PC-SAFT EoS is able to estimate VLE well using the parameter set obtained from the density measurements in the homogeneous region. In contrast, VLE estimated by SL EoS is lower than the actual measurements. It might be concluded that the parameter sets determined from the density measurements can be applied for the estimation of other properties such as VLE, with SL and PC-SAFT EoS because of the origins of the model.

3.4. Estimation of isochore (equal density line) with EoS

In Fig. 8, isochores are drawn using SL EoS, PC-SAFT EoS, and density equation. In the VLE diagram, the isochore is represented by a curve with a minimum value. As the density increases, the minimum value shifts to the high-pressure side, to a CO_2 composition around 0.5. Comparing the isochores obtained by estimation from the two EoS, the results on the high CO_2 composition side

Table 3
Densities of the CO_2(1)/Tol(2) system (pressure P, density ρ, CO_2 mole fraction x_1, and the combined standard uncertainties in experimental density u_c and composition u_x).[a,b]

313.15 K			333.15 K			353.15 K		
Pressure/MPa	Density/kg m^{-3}	Uncertainties u_c/kg m^{-3}	Pressure/MPa	Density/kg m^{-3}	Uncertainties u_c/kg m^{-3}	Pressure/MPa	Density/kg m^{-3}	Uncertainties u_c/kg m^{-3}
x_1 = 0								
20.01	864.0	0.22	19.94	847.1	0.22	19.92	829.8	0.22
18.94	863.2	0.22	19.00	846.3	0.22	18.99	829.0	0.22
17.95	862.5	0.22	18.04	845.5	0.22	17.99	828.1	0.22
16.96	861.8	0.22	16.98	844.6	0.22	17.01	827.2	0.22
16.01	861.1	0.22	15.99	843.8	0.22	16.00	826.3	0.22
15.04	860.3	0.22	15.00	843.0	0.22	15.02	825.3	0.22
14.03	859.6	0.22	14.07	842.2	0.22	14.01	824.5	0.22
13.03	858.8	0.22	13.05	841.4	0.22	13.04	823.6	0.23
12.09	858.2	0.22	12.09	840.5	0.22	12.07	822.7	0.23
11.06	857.4	0.22	11.02	839.6	0.22	11.04	821.7	0.23
10.11	856.6	0.22	10.07	838.7	0.22	10.03	820.6	0.23
9.05	855.8	0.22	8.95	837.7	0.22	8.97	819.6	0.23
8.10	855.1	0.22	7.96	836.9	0.22	7.98	818.6	0.23
6.88	854.2	0.22	6.99	836.0	0.23	7.06	817.7	0.23
6.03	853.5	0.22	6.04	835.0	0.23	6.04	816.5	0.23
5.00	852.6	0.22	5.05	834.1	0.23	5.05	815.5	0.24
3.94	851.6	0.22	4.01	833.2	0.23	4.05	814.5	0.24
2.93	850.8	0.22	2.98	832.2	0.23	3.06	813.4	0.24
2.04	850.1	0.22	2.09	831.3	0.23	2.06	812.3	0.24
0.99	849.2	0.22	1.04	830.3	0.23	1.14	811.3	0.24
x_1 = 0.2000 (u_x = 0.0010)								
19.94	873.9	0.23	19.96	854.8	0.23	19.97	834.1	0.24
18.92	872.9	0.23	18.92	853.8	0.23	18.98	832.9	0.24
17.90	872.0	0.23	17.97	852.7	0.23	18.01	831.8	0.24
17.01	871.2	0.23	16.92	851.7	0.23	17.05	830.7	0.24
16.03	870.3	0.23	16.00	850.7	0.24	16.03	829.5	0.25
15.03	869.4	0.23	15.05	849.7	0.24	15.05	828.2	0.25
14.03	868.5	0.23	14.07	848.7	0.24	14.06	827.0	0.25
13.10	867.6	0.23	13.07	847.7	0.24	13.03	825.8	0.25
12.06	866.6	0.23	12.05	846.5	0.24	12.07	824.6	0.26
11.08	865.7	0.22	11.06	845.4	0.24	11.03	823.4	0.26
10.07	864.7	0.22	10.06	844.3	0.24	10.01	822.0	0.26
9.11	863.8	0.22	9.05	843.2	0.24	9.08	820.8	0.27
8.05	862.7	0.22	7.96	841.9	0.24	8.01	819.4	0.27
6.86	861.5	0.22	6.91	840.6	0.24	6.97	818.0	0.27
6.02	860.8	0.22	6.07	839.5	0.25	6.02	816.7	0.28
5.04	859.8	0.22	5.09	838.3	0.25	5.03	815.4	0.28
4.01	858.7	0.22	4.07	837.0	0.25	4.05	813.9	0.28
2.97	857.7	0.22	3.02	835.8	0.25			
x_1 = 0.4024 (u_x = 0.0007)								
19.99	883.6	0.28	20.03	859.4	0.25	20.07	833.9	0.24
18.96	882.4	0.27	19.02	858.0	0.26	19.06	832.3	0.24
17.98	881.3	0.27	18.03	856.7	0.26	18.05	830.6	0.25
17.00	880.1	0.27	17.08	855.3	0.26	17.05	829.0	0.25
16.00	878.8	0.27	16.07	853.9	0.26	16.07	827.4	0.26
14.96	877.6	0.27	15.06	852.5	0.27	15.09	825.7	0.26
14.02	876.4	0.27	14.07	851.0	0.27	14.05	823.8	0.27
13.03	875.2	0.27	13.12	849.6	0.27	13.03	822.0	0.27
12.05	873.9	0.27	11.94	847.7	0.27	11.99	820.1	0.28
11.06	872.7	0.27	11.05	846.3	0.28	10.96	818.1	0.29
10.07	871.4	0.27	9.99	844.6	0.28	9.99	816.3	0.29
9.12	870.1	0.27	9.05	843.1	0.28	8.99	814.2	0.30
8.02	868.6	0.27	7.98	841.4	0.28	7.98	812.1	0.30
6.98	867.1	0.27	6.98	839.6	0.29			
6.04	865.9	0.26	6.05	838.1	0.29			
4.99	864.4	0.26						
x_1 = 0.6000 (u_x = 0.0005)								
19.90	889.7	0.37	19.96	858.6	0.31	20.03	824.6	0.27
19.00	888.2	0.37	19.00	856.6	0.32	19.02	822.0	0.28
17.96	886.5	0.37	18.02	854.5	0.32	18.04	819.5	0.29
17.05	884.9	0.37	16.99	852.4	0.33	17.06	816.9	0.30
16.04	883.1	0.36	15.94	850.1	0.34	16.05	814.1	0.31
15.05	881.4	0.36	15.05	848.1	0.34	15.06	811.2	0.32
14.08	879.7	0.36	14.07	845.8	0.35	14.04	808.3	0.34
13.05	877.8	0.36	13.05	843.4	0.35	13.07	805.3	0.35
12.05	875.9	0.36	12.06	841.1	0.36	12.02	801.9	0.36
11.09	874.1	0.36	10.95	838.1	0.36	11.04	798.6	0.37
10.03	872.0	0.36	10.08	836.0	0.37			
9.04	870.0	0.35	8.97	833.0	0.37			

(*continued on next page*)

Table 3 (*continued*)

313.15 K			333.15 K			353.15 K		
Pressure/MPa	Density/kg m^{-3}	Uncertainties u_c/kg m^{-3}	Pressure/MPa	Density/kg m^{-3}	Uncertainties u_c/kg m^{-3}	Pressure/MPa	Density/kg m^{-3}	Uncertainties u_c/kg m^{-3}
8.02	867.8	0.35						
6.84	865.4	0.35						
x_1 = 0.8000 (u_x = 0.0005)								
20.08	890.2	0.45	19.98	839.9	0.49	19.97	782.8	0.70
18.98	887.0	0.46	19.00	835.8	0.51	19.05	777.3	0.75
18.04	884.1	0.46	18.04	831.6	0.52	18.05	770.8	0.79
17.04	880.9	0.46	17.02	827.0	0.54	17.04	763.9	0.84
16.02	877.5	0.47	16.03	822.2	0.56	16.06	756.3	0.88
15.06	874.2	0.47	15.07	817.2	0.58	15.04	747.9	0.93
14.08	870.7	0.48	14.04	811.6	0.60	14.02	738.3	0.97
13.13	867.2	0.48	13.08	806.0	0.62	13.00	726.8	1.02
12.04	863.0	0.49	12.07	799.6	0.63			
11.07	859.1	0.50	11.04	792.3	0.65			
10.06	854.8	0.50						
9.07	850.3	0.51						
8.00	845.1	0.52						

[a] Standard uncertainties u are $u(T)$ = 0.15 K, $u(P)$ = 0.033 MPa.
[b] Under all the conditions, the mixture was in the compressed uniform liquid phase state.

Table 4
Parameters in the density equation (fitting parameters *a*, *b*, *c*, *m*, *n*, *k*, *A*, *B*, and *C*).

T (K)	*a*	*b*	*c*	*m*	*n*	*k*	*A*	*B*	*C*	*AARD* (%)
313	21.81	20.18	0.03228	2.068	11.65	4.432	6.492	1.682	1.434	0.13
333	32.47	21.29	−32.55	6.42699	5.186	4.164	6.008	1.087	1.241	0.23
353	15.80	304.7	−599.5	201.9	−196.3	4.433	6.275	1.298	1.212	0.07

Table 5
Results from the density correlations for the CO_2(1)/Tol(2) system with three EoS.

T/K	PR EoS			SL EoS		PC-SAFT EoS	
	k_{12}	l_{12}	*AARD*/%	δ_{12}	*AARD*/%	θ_{12}	*AARD*/%
313	0.442	0.254	3.30	0.015	0.27	0.107	0.43
333	0.374	0.243	3.33	−0.001	0.17	0.111	0.32
353	0.319	0.233	3.34	−0.010	0.14	0.118	0.37

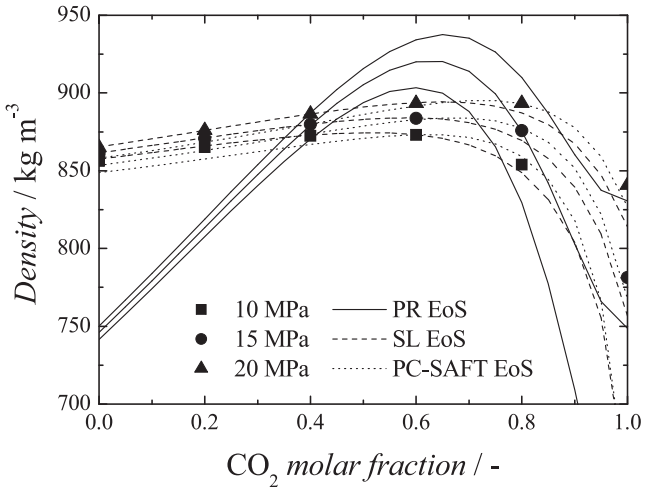

Fig. 7. Correlation results of the densities at 313 K with the PR, SL, and PC-SAFT EoS.

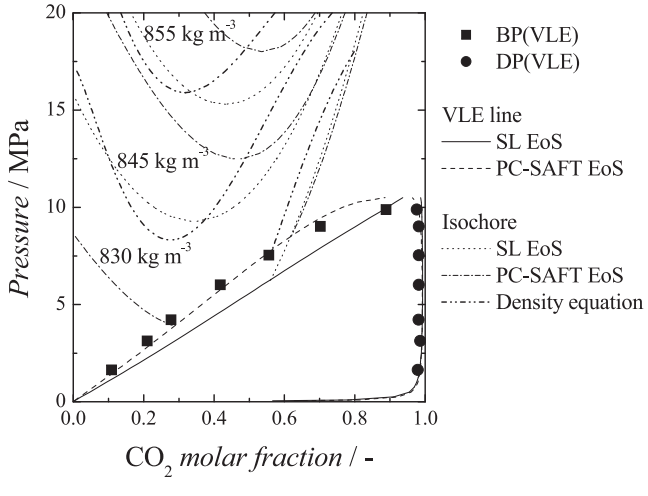

Fig. 8. Estimation of the vapor–liquid phase diagram at 333 K with the SL and PC-SAFT EoS [8].

are consistent, whereas on the low CO_2 composition side, the results from SL EoS are on the lower pressure side. In contrast, the isochore estimation from the density equation is rather close to the results from SL EoS. The difference in the density correlation accuracy shown in Table 5 and Fig. 7 significantly affects the isochore determination. As mentioned above, the pure component

Table 6
Estimation of the vapor-liquid equilibrium lines for the CO_2(1)/Tol(2) system using three EoS with interaction parameters obtained by the density correlations.

T/K	AARD/%			Number of data points
	PR EoS	SL EoS	PC-SAFT EoS	
313	28.66	6.69	2.19	5 (from Ref. [42])
333	38.28	24.45	9.25	7 (from Ref. [8])
353	82.31	32.95	9.04	12 (from Ref. [44])

parameters of the PC-SAFT EoS are obtained by correlating the liquid density and saturated vapor pressure. Therefore, the density estimation accuracy is somewhat inferior, in this case, which could explain the divergent results.

3.5. Estimation of density with EoS

Unlike the results reported in Sections 3.3. and 3.4, the densities of the CO_2/Tol system were estimated using each of the EoS with interaction parameters obtained from the VLE correlations, to optimize Eq. (35). The correlation results for VLEs are tabulated in Table 7. From the table, the *AARD* decreases in the following order: PC-SAFT EoS > SL EoS > PR EoS. However, all the EoS correlate well with VLE. The estimated density results are shown in Table 8 and Fig. 9. It can be seen from Fig. 9 that the results obtained for the PR EoS is lower overall than the actual measurements. Comparing Figs. 7 and 9, although the results for SL EoS at high CO_2 compositions are slightly inferior, the correlation and estimation line are almost identical for SL and PC-SAFT EoS. Further, as seen from Tables 5 and 7, the interaction parameters are nearly identical for the correlation and estimation data. Based on the estimation results for VLE in Section 3.3, the interaction parameter value obtained for SL EoS is considered to be sensitive to VLE, because the calculated results differ even with a small change in the values.

4. Conclusion

The densities of homogeneous fluid mixtures of the CO_2/Tol system were measured over a wide range of temperature, pressure, and compositions using a high-pressure vibration-type density meter. In general, the density trends were similar to those reported in previous works. The experimental results correlated well with the density function based on the Tait equation, with an *AARD* of less than 0.22%. The experimental results were also fit to three different EoS, namely PR, SL, and PC-SAFT EoS, and the individual parameter sets were determined for each EoS. The PR EoS was found to be unreliable for density correlations. With the determined parameter sets, VLE and isochore were estimated using SL and PC-SAFT EoS. While the estimation of VLE with the PC-SAFT EoS was more accurate than SL EoS, the results for isochore were inferior for the PC-SAFT EoS. This is mostly attributed to the differences in the pure component parameters used in each EoS. A parameter set was determined from the density measurements carried out in the homogeneous region of the mixtures and used to estimate the VLE of the mixtures. The SL and PC-SAFT EoS from which these parameters were determined based on density and/or vapor pressure, were suitable for correlating the density and estimating the VLE of the mixtures. This was presumably due to the fact that these EoS not only account for the association term, but also the repulsive term in the intermolecular interactions. The use of a parameter set determined from VLE to estimate the density was also examined, and SL and PC-SAFT EoS were found to be suitable for these calculations. For the density calculations, SL EoS was the most suitable, followed by PC-SAFT EoS. In studying the efficient estimation of a wide variety of physical properties, it becomes clear that the basic data used for determining the pure component parameters is of primary importance for calculating density values. The CO_2/Tol system did not need to take into account the association of molecules, and the SL EoS is formulated based on the assumption of random mixing without considering association. Thus, this result would be expected to be different if

Table 8
Estimation of the density for the CO_2(1)/Tol(2) system using three EoS with interaction parameters obtained by the vapor-liquid equilibrium line correlations.

T/K	AARD/%		
	PR EoS	SL EoS	PC-SAFT EoS
313	10.34	0.44	0.46
333	12.46	1.02	0.40
353	12.96	1.28	0.45

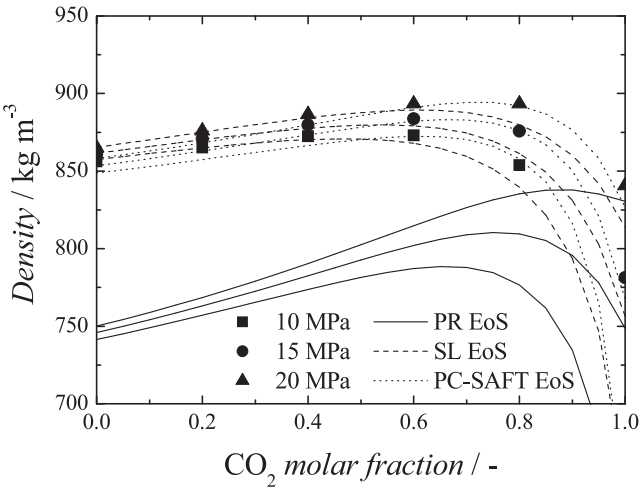

Fig. 9. Estimation of the densities at 313 K with the PR, SL, and PC-SAFT EoS.

Table 7
Results from the vapor-liquid equilibrium line correlations for the CO_2(1)/Tol(2) system using three EoS.

T/K	PR EoS			SL EoS		PC-SAFT EoS		Number of data points
	k_{ij}	l_{ij}	AARD/%	δ_{ij}	AARD/%	θ_{ij}	AARD/%	
313	0.113	0.004	0.42	0.031	1.76	0.104	0.70	5 (from Ref. [42])
333	0.116	−0.030	1.52	0.039	2.09	0.117	8.02	7 (from Ref. [8])
353	0.115	−0.036	1.39	0.034	3.24	0.123	8.11	12 (from Ref. [44])

the molecules do in fact, associate. Therefore, in the future, studies are needed to measure associated molecules such as methanol to verify the effects of association on the correlation and estimation accuracy using EoS.

Declaration of Competing Interest

The authors declare that they have no known competing financial interests or personal relationships that could have appeared to influence the work reported in this paper.

References

[1] Y. Takeshita, Y. Sato, S. Nishi, Ind. Eng. Chem. Res. 39 (2000) 4496–4499.
[2] S.-Y. Wang, N.-L. Wu, J. Non-Cryst. Solids 224 (1998) 259–266.
[3] A. Sane, J. Limtrakul, The Journal of Supercritical Fluids 51 (2009) 230–237.
[4] A.V. Pripakhaylo, R.N. Magomedov, T.A. Maryutina, J. Anal. Chem. 74 (2019) 401–409.
[5] M. Lazrag, E. Steiner, C. Lemaitre, F. Mutelet, R. Privat, S. Rode, A. Hannachi, D. Barth, J. Sol-Gel Sci. Technol. 84 (2017) 453–465.
[6] M.L. Williams, J.S. Dickmann, J.C. Hassler, E. Kiran, Ind. Eng. Chem. Res. 56 (2017) 8748–8766.
[7] E. Kiran, W. Zhuang, Y.L. Sen, J. Appl. Polym. Sci. 47 (1993) 895–909.
[8] K. Tochigi, K. Hasegawa, N. Asano, K. Kojima, J. Chem. Eng. Data 43 (1998) 954–956.
[9] D.-Y. Peng, D.B. Robinson, Ind. Eng. Chem. Res. 15 (1976) 59–64.
[10] M. Zirrahi, B. Azinfar, H. Hassanzadeh, J. Abedi, J. Chem. Eng. Data 60 (2015) 1592–1599.
[11] H. Matsukawa, K. Kuwabara, Y. Shimada, T. Tsuji, K. Otake, J. Chem. Thermodyn. 142 (2020) 105902–106022.
[12] E. Moine, A. Piña-Martinez, J.-N. Jaubert, B. Sirjean, R. Privat, Ind. Eng. Chem. Res. 58 (2019) 20815–20827.
[13] G. Soave, Chem. Eng. Sci. 27 (1972) 1197–1203.
[14] J. Gross, G. Sadowski, Ind. Eng. Chem. Res. 40 (2001) 1244–1260.
[15] J. Gross, G. Sadowski, Ind. Eng. Chem. Res. 41 (2002) 5510–5515.
[16] L. Verlet, Phys. Rev. 165 (1968) 201–214.
[17] K. Fukuchi, Y. Koga, Y. Arai, Netsu Bussei 7 (1992) 21–25.
[18] O. Pfohl, T. Giese, R. Dohrn, G. Brunner, Ind. Eng. Chem. Res. 37 (1998) 2957–2965.
[19] J.-N. Jaubert, R. Privat, Y.L. Guennec, L. Coniglio, Fluid Phase Equilib. 419 (2016) 88–95.
[20] R. Privat, J.-N. Jaubert, Y.L. Guennec, Fluid Phase Equilib. 427 (2016) 414–420.
[21] R.R. Mallepally, B.A. Bamgbade, N. Cain, M.A. McHugh, Fluid Phase Equilib. 449 (2017) 138–147.
[22] R.A. Krenz, T. Laursen, R.A. Heidemann, Ind. Eng. Chem. Res. 48 (2009) 10664–10681.
[23] N. Koak, R.A. Heidemann, Ind. Eng. Chem. Res. 35 (1996) 4301–4309.
[24] R.H. Lacombe, I.C. Sanchez, J. Phys. Chem. 80 (1976) 2568–2580.
[25] I.C. Sanchez, R.H. Lacombe, J. Phys. Chem. 80 (1976) 2352–2362.
[26] I.C. Sanchez, R.H. Lacombe, Macromolecules 11 (1978) 1145–1156.
[27] M. Kato, D. Kodama, T. Ono, M. Kokubo, J. Chem. Eng. Data 54 (2009) 2953–2956.
[28] E.C. Ihmels, J. Gmehling, Ind. Eng. Chem. Res. 40 (2001) 4470–4477.
[29] H. Matsukawa, Y. Shimada, S. Yoda, Y. Okawa, M. Naya, A. Shono, K. Otake, Fluid Phase Equilib. 455 (2018) 6–14.
[30] M.L. Michelsen, H. Kistenmacher, Fluid Phase Equilib. 58 (1990) 229–230.
[31] B.E. Poling, J.M. Prausnitz, J.P. O'Connell, The Properties of Gases and Liquids, McGraw-Hill Proffesional, 2001.
[32] Y. Xiong, E. Kiran, Polymer 35 (1994) 4408–4415.
[33] D. Sommer, R. Kleinrahm, R. Span, W. Wagner, J. Chem. Thermodyn. 43 (2011) 117–132.
[34] G. Watson, T. Lafitte, C.K. Zéberg-Mikkelsen, A. Baylaucq, D. Bessieres, C. Boned, Fluid Phase Equilib. 247 (2006) 121–134.
[35] N.F. Glen, A.I. Johns, J. Chem. Eng. Data 54 (2009) 2538–2545.
[36] R. Span, W. Wagner, J. Phys. Chem. Ref. Data 25 (1996) 1509–1596.
[37] N. Falco, E. Kiran, The Journal of Supercritical Fluids 61 (2012) 9–24.
[38] M. Chorzewski, J.-P.E. Grolier, S.L. Randzio,, J. Chem. Eng. Data 55 (2010) 5489–5496.
[39] H. Pöhler, E. Kiran, J. Chem. Eng. Data 41 (1996) 482–486.
[40] J. Wu, Q. Pan, G.L. Rempel, J. Chem. Eng. Data 49 (2004) 976–979.
[41] Y. Sanchez-Vicente, W.J. Tay, S.Z. Al Ghafri, E.C. Efika, J.P.M. Trusler, Ind. Eng. Chem. Res. 59 (2020) 7224–7237.
[42] A. Bondi, The Journal of Physical Chemistry 68 (1964) 441–451.
[43] E.N. Lay, J. Chem. Eng. Data 55 (2010) 223–227.
[44] W. Wu, J. Ke, M. Poliakoff, J. Chem. Eng. Data 51 (2006) 1398–1403.
[45] W.O. Morris, M.D. Donohue, J. Chem. Eng. Data 30 (1985) 259–263.
[46] Y. Adachi, B.C.-Y. Lu, THe Canadian Journal of Chemical Engineering 63 (1985) 497–503.

JCT D-21-00167